Journal of Biomechanics 42 (2009) 1270–1274

Contents lists available at ScienceDirect

Journal of Biomechanics

journal homepage: www.elsevier.com/locate/jbiomech
www.JBiomech.com

Dynamic behaviors of microtubules in cytosol

C.Y. Wang *, C.F. Li, S. Adhikari

School of Engineering, Swansea University, Singleton Park, Swansea SA2 8PP, Wales, UK

ARTICLE INFO

Article history:
Accepted 10 March 2009

Keywords:
Microtubules
Cytosol
Orthotropic shells
Stokes flow
Vibration

ABSTRACT

Highly anisotropic microtubules (MTs) immersed in cytosol are a central part of the cytoskeleton in eukaryotic cells. The dynamic behaviors of an MT–cytosol system are of major interest in biomechanics community. Such a solid–fluid system is characterized by a Reynolds number of the order 10^{-3} and a slip ionic layer formed at the MT–cytosol interface. In view of these unique features, an orthotropic shell-Stokes flow model with a slip boundary condition has been developed to explore the distinctive dynamic behaviors of MTs in cytosol. Three types of motions have been identified, i.e., (a) undamped and damped torsional vibration, (b) damped longitudinal vibration, and (c) overdamped bending and radial motions. The exponentially decaying bending motion given by the present model is found to be in qualitative agreement with the existing experimental observation [Felgner et al., 1996. Flexural rigidity of microtubules measured with the use of optical tweezers, Journal of Cell Science 109, 509–516].

1. Introduction

Microtubules (MTs) (Fig. 1) are principle components of the cytoskeleton in eukaryotic cells, which play an essential role in providing mechanical rigidity, maintaining the shape of cells and facilitating many important physiological processes (Ingber et al., 1995; Nogales, 2000; Cotterill, 2002; Boal, 2002; Howard and Hyman, 2003; Stamenovic, 2005; Watanabe et al., 2005). The mechanics of MTs is a topic of numerous researches (Gittes et al., 1993; Venier et al., 1994; Kurachi et al., 1995; Felgner et al., 1996; dePablo et al., 2003), where MT vibration is of major interest (Sirenko et al., 1996; Pokorny, 2003, 2004; Kasas et al., 2004; Portet et al., 2005; Wang and Zhang, 2008). In particular, since MTs are immersed in cytosol, the vibration of MTs in a fluid has attracted attention in the last decade (Sirenko et al., 1996; Pokorny, 2003 2004). In studying the longitudinal vibration, Pokorny (2003, 2004) revealed that an ionic charge layer on the surfaces of MTs minimizes the viscous effect of the cytosol and allows slide between MTs and cytosol. The more comprehensive investigation has been carried out by Sirenko et al. (1996), where three axisymmetric acoustic modes and an infinite set of non-axisymmetric modes have been obtained. In this study, an isotropic membrane shell model is used for MTs and the fluid around MTs is tacitly assumed to be an ideal fluid with an infinitely large Reynolds number. However, such a model is oversimplified for anisotropic MTs with bending resistance. Furthermore, as will be shown later, the nanoscale radius of MTs gives a Reynolds number of the surrounding fluid three orders of magnitude smaller than unity. The ideal fluid model is thus not valid for an MT–fluid system. It follows that a more realistic model for an MT–cytosol system is needed to give a reliable description of the dynamic behaviors of MTs immerged in cytosol.

Recently, an orthotropic shell model (Wang et al., 2006a,b; Wang and Zhang, 2008) has been developed to study the mechanical behaviors of MTs. A good agreement has been achieved between this shell model, available discrete models and experiments. Motivated by its valid applications, the present paper will further extend the model to the vibration analysis of an MT–cytosol system. The motion of the cytosol will be modeled as Stokes flow characterized by a small Reynolds number and the free slip boundary condition will be specified on the MT surface.

Based on this orthotropic shell-Stokes flow model, the governing equations for the vibration of MTs in cytosol are derived in Section 2. In Section 3, the phonon-dispersion relations are predicted for MTs immersed in cytosol and compared with those of free MTs. Here the major attention is focused on the damping effect of cytosol on various MT motions. The major conclusions are summarized in Section 4.

2. The orthotropic shell-Stokes flow model

In this section, we shall develop an orthotropic shell-Stokes flow model for the dynamic behaviors of MTs in cytosol.

2.1. Dynamic equations of MTs

An orthotropic shell model developed for the free vibration (Wang et al., 2006a; Wang and Zhang, 2008) and elastic buckling

* Corresponding author. Tel.: +44 1792 602825; fax: +44 1792 295676.
E-mail address: chengyuan.wang@swansea.ac.uk (C.Y. Wang).

0021-9290/$ - see front matter © 2009 Elsevier Ltd. All rights reserved.
doi:10.1016/j.jbiomech.2009.03.027

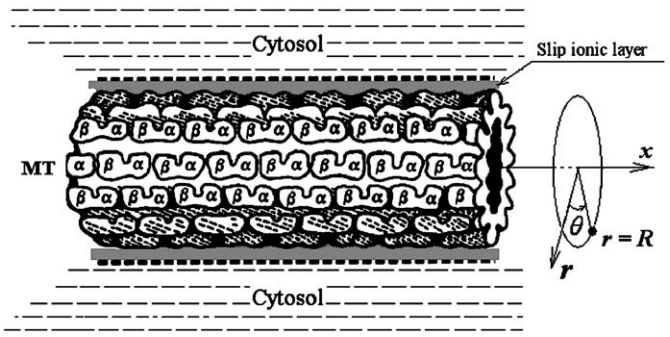

Fig. 1. A schematic picture of an MT immerged in cytosol with a slip ionic layer at the MT–cytosol interface. α and β are tubulin dimers that form MTs.

(Wang et al., 2006b) of MTs will be further used to study the dynamic behaviors of MTs in cytosol. Previous studies (Pokorny, 2003, 2004) indicated that the viscous force on MTs is minimized by a slip ionic layer formed at the MT–cytosol interface (Fig. 1). The friction acting on MT surface is thus neglected in the present study. On the other hand, the inner radial pressure $P_{rr}{}^{i}$ and the outer radial pressure $P_{rr}{}^{o}$ of MTs due to cytosol have to be considered. The dynamic equations of MTs in cytosol can then be written as follows (Wang et al., 2006a; Wang and Zhang, 2008):

$$\left\{R^2\frac{\partial^2}{\partial x^2}+\frac{K_{x\theta}R^2+D_{x\theta}}{K_xR^2}\frac{\partial^2}{\partial\theta^2}\right\}u+\left\{\frac{(v_xK_\theta+K_{x\theta})R}{K_x}\frac{\partial^2}{\partial x\partial\theta}\right\}\times v+\left\{-\frac{v_xK_\theta R}{K_x}\frac{\partial}{\partial x}+\frac{D_xR}{K_x}\frac{\partial^3}{\partial x^3}-\frac{D_{x\theta}}{K_xR}\frac{\partial^3}{\partial x\partial\theta^2}\right\}\times w=\frac{\rho h}{K_x}R^2\frac{\partial^2u}{\partial t^2}$$

$$\left\{\left(v_\theta+\frac{K_{x\theta}}{K_x}\right)R\frac{\partial^2}{\partial x\partial\theta}\right\}u+\left\{\frac{K_\theta}{K_x}\frac{\partial^2}{\partial\theta^2}+\frac{K_{x\theta}R^2+3D_{x\theta}}{K_x}\frac{\partial^2}{\partial x^2}\right\}\times v+\left\{-\frac{K_\theta}{K_x}\frac{\partial}{\partial\theta}+\frac{v_\theta D_x+3D_{x\theta}}{K_x}\frac{\partial^3}{\partial x^2\partial\theta}\right\}\times w=\frac{\rho h}{K_x}R^2\frac{\partial^2v}{\partial t^2}$$

$$\left\{v_\theta R\frac{\partial}{\partial x}-\frac{D_x}{K_x}R\frac{\partial^3}{\partial x^3}+\frac{D_{x\theta}}{K_xR}\frac{\partial^3}{\partial x\partial\theta^2}\right\}\times u+\left\{\frac{K_\theta}{K_x}\frac{\partial}{\partial\theta}-\frac{v_xD_\theta+3D_{x\theta}}{K_x}\frac{\partial^3}{\partial x^2\partial\theta}\right\}\times v+\left\{-\frac{D_x}{K_x}R^2\frac{\partial^4}{\partial x^4}-\frac{v_xD_\theta+v_\theta D_x+4D_{x\theta}}{K_x}\frac{\partial^4}{\partial x^2\partial\theta^2}-\frac{D_\theta}{K_xR^2}\left(\frac{\partial^2}{\partial\theta^2}+1\right)^2-\frac{K_\theta}{K_x}\right\}\times w+\frac{R^2}{K_x}(P_{rr}^{i}-P_{rr}^{o})=\frac{\rho h}{K_x}R^2\frac{\partial^2w}{\partial t^2}\quad(1)$$

where x and θ are axial and circumferential angular coordinates (Fig. 1); u, v and w are axial, circumferential and radial displacements; t is the time; ρ is the mass density, h is the thickness and R is the average radius of MTs. In addition, v_x and v_θ are Poisson ratios in longitudinal and circumferential directions. (K_x, K_θ) and (D_x, D_θ) represent the in-plane and bending stiffnesses in longitudinal and circumferential directions, and ($K_{x\theta}$, $D_{x\theta}$) are stiffnesses in shear (Appendix A1). Here we consider MTs usually of a large length-to-diameter aspect ratio as infinitely long shells. The solution of Eq. (1) then reads (Sirenko et al., 1996)

$$\begin{bmatrix}u(x,\ \theta,\ t)\\ v(x,\ \theta,\ t)\\ w(x,\ \theta,\ t)\end{bmatrix}=\begin{bmatrix}U\\ V\\ -iW\end{bmatrix}\exp(in\theta+ik_xx-i\omega t)\quad(2)$$

where U, V and W represent the vibration amplitudes of MTs in longitudinal, circumferential and radial directions, k_x is the wave vector (nm^{-1}) along the longitudinal direction, n is the circumferential wave number and the real part of ω (Re ω) gives the angular frequency.

2.2. Dynamic equations of cytosol motion

The radius R of MTs is around 10 nm and their free vibration frequency f with $k<0.1$ ($k=Rk_x$) is of the order 0.1 GHz (Wang et al., 2006a). If the displacement amplitude Amp of MT vibration is 10 times smaller than MT radius, the velocity of the cytosol flow can be roughly estimated as $\tilde{v}=4\,\text{Amp}\times f=0.4$ m/s. Since water is a major part (70%) of cytosol, its kinematic viscosity $\eta=1.004\times10^{-6}\,m^2/s$ (at 20 °C) should be close to that of cytosol. Thus, the Reynolds number of cytosol $Re=vR/\eta$ is of the order 4.0×10^{-3}. It follows that the motion of cytosol can be modeled as Stokes flow, i.e., an incompressible fluid with small Reynolds number (<1), whose governing equations are as follows (Happel and Brenner, 1973):

$$\nabla\bullet\tilde{v}_f=0\quad\text{and}\quad\nabla p_f=\mu_f\nabla^2\tilde{v}_f\quad(3)$$

where $\tilde{v}_f$ denotes the velocity, p_f the pressure and μ_f the dynamical viscosity of cytosol.

The continuity condition requires that cytosol moves radially with the same velocity as that of MTs at $r=R$. However, due to the existence of a very thin slip ionic layer on MT surfaces, MTs and cytosol move independently along the longitudinal and circumferential directions. In fact, as there is no friction between the MTs and the thin slip layer with negligible momentum and angular momentum of inertia, the viscous force between the cytosol and the slip ionic layer must also be zero. It follows that the tangential velocities of cytosol should vanish at $r=R$. Thus, the boundary conditions of cytosol at $r=R$ are

$$(\tilde{v}_f)_x=0,\ (\tilde{v}_f)_\theta=0\quad\text{and}\quad(\tilde{v}_f)_r=-\frac{\partial w}{\partial t}\quad(4)$$

By using the governing Equation (3) and boundary condition (4), the radial pressures $P_{rr}{}^{i}$ and $P_{rr}{}^{o}$ of cytosol at the inner and outer surfaces of MTs can be expressed as

$$\begin{bmatrix}P_{rr}^{i}\\ P_{rr}^{o}\end{bmatrix}=-\begin{bmatrix}A^i(n,\ k)\\ A^o(n,\ k)\end{bmatrix}\frac{\mu_f\,\omega\,W\exp(in\theta+ik_xx-i\omega t)}{R}\quad(5)$$

The derivation of Eq. (5) and the form of A^i and A^0 can be found in Appendix B.

2.3. Dynamic analysis of MTs in cytosol

By substituting Eqs. (2) and (5) into (1), the original partial differential can be transformed into the following three algebraic equations:

$$\{k^2+\beta(1+\gamma)n^2-\Omega^2\}U+\{-(\alpha v_x+\beta)kn\}\times V+\{\alpha v_xk+\gamma(k^2-\beta n^2)k\}W=0$$

$$\{(\alpha v_x+\beta)kn\}U+\{\alpha n^2+\beta(1+3\gamma)k^2-\Omega^2\}\times V+\left\{\alpha n+\gamma(\alpha v_x+3\beta)k^2n\right\}W=0$$

$$\{\alpha v_x k+\gamma(k^2-\beta n^2)k\}U+\{\alpha n+\gamma(\alpha v_x+3\beta)k^2 n\}\times V+\{\gamma k^4+2\gamma(\alpha v_x+2\beta)k^2 n^2+\alpha\gamma(n^2-1)^2+\alpha-(\Omega^2-M_{nk}\Omega)\}W=0 \quad (6)$$

where Ω ($\Omega=R\omega/S_L$) is a dimensionless frequency quantity ($S_L=\sqrt{E_x/\rho}$ and E_x is an axial Young's modulus), $M_{nk}=-i\mu_f/h\sqrt{\rho E_x}(A^o(n,k)-A^i(n,k))$is the equivalent damping coefficient of cytosol, α and β (Appendix A2) describe the anisotropic characters of MTs, and $\gamma=D_x/k_x$. The existence condition of a nonzero solution of U, V and W is

$$\det H(n,\ k,\ \Omega)_{3\times 3}=0 \quad (7)$$

where H is the coefficient matrix of Eq. (6). Solving Eq. (7), one can obtain Ω as a function of n and k for MTs submerged in cytosol. Substituting the value of Ω into Eq. (7) yields the amplitude ratio (U/W, V/W, 1), which defines the associated vibration modes of MTs.

3. Results and discussions

Proceeding in the way demonstrated in Section 2, we shall study the dynamic behaviors of MTs immersed in cytosol. The values of material constants used here are in Appendix A3.

3.1. Axisymmetric vibration of MTs

In this section we shall focus on the axisymmetric vibration of MTs where the circumferential wave number $n=0$. In this case the displacements of MTs are uniformly distributed along the circumference independent of θ. The phonon-dispersion curves have been calculated in Fig. 2 for MTs in cytosol (solid lines) and compared with those of free MTs (dotted lines). In Fig. 2, free MTs show longitudinal (L) and torsional (T) modes characterized by a linear dispersion law and a radial (R) mode whose frequency approaches an asymptotic value when k goes to zero. When cytosol is introduced, it is seen from Fig. 2 that an MT–cytosol system only supports L and T modes, whose phonon-dispersion curves coincide with their counterparts of free MTs. In contrast, the R mode observed for free MTs vanishes.

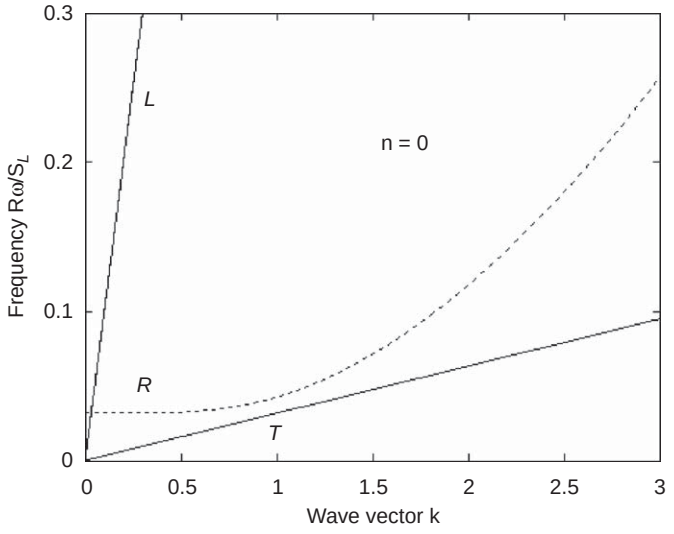

Fig. 2. The phonon-dispersion curves for axisymmetric modes of free MTs (dotted lines) and MTs in cytosol (solid lines). *L*: longitudinal mode, *T*: torsional mode, *R*: radial mode. Here, the dotted lines for *L* and *T* modes of free MTs coincide with their solid counterparts obtained for MTs in cytosol.

It is easy to see that at $n=0$, the second equation of Eq. (6) reduces to

$$\{\beta(1+3\gamma)k^2-\Omega^2\}V=0 \quad (8)$$

which is decoupled with other two equations of Eq. (6). It thus gives a pure torsional vibration of MTs with a linear dispersion relation $\Omega\approx 0.032k$ (see Fig. 2). Obviously, the damping coefficient M_{nk} has no effect on such a vibration which is decoupled with a radial motion. The axisymmetric T mode in cytosol is thus a free vibration without damping.

The first and third equations of Eq. (6) with $n=0$ form Eq. (9), which describes the vibration modes where longitudinal and radial displacements are coupled via v_x and γ

$$\begin{bmatrix} k^2-\Omega^2 & \alpha v_x k+k^3\gamma \\ \alpha v_x k+k^3\gamma & k^4\gamma+\alpha(\gamma+1)-(\Omega^2-M_{nk}\Omega)\end{bmatrix}\begin{bmatrix} U \\ W\end{bmatrix}=0 \quad (9)$$

Here let us first consider small k, e.g., $k<0.1$. Bearing in mind that α, γ and $k\ll 1$, the following approximate equation can be obtained based on Eqs. (9) and (7)

$$(\Omega^2-k^2)(\Omega^2-M_{nk}\Omega-\alpha)=0 \quad (10)$$

A linear dispersion relation $\Omega=k$ can be derived, which corresponds to L mode (Fig. 2) in the limit of small k, i.e., extremely large axial wavelength λ ($=2\pi R/k$). In this case, MTs behave like elastic columns where L mode is almost decoupled with the radial one. Thus, damping of such an L mode can almost be neglected. On the other hand, in general case the axisymmetric L mode of elastic shells is still coupled with a small radial motion. In this case the exact solution given by condition (7) for Eq. (9) is $\Omega=A-Bi$ where A and B are positive real numbers. Recall Eq. (2) and replace ω with $S_L\Omega/R$ the longitudinal vibration can be expressed as

$$u(x,\ \theta,\ t)=(Ue^{(-BS_L/R)t})\exp(in\theta+ik_x x-i\frac{AS_L}{R}t) \quad (11)$$

It is clearly seen from Eq. (11) that A gives the frequency quantity shown in Fig. 2 and $-B$ quantifies the damping effect of cytosol on the L mode, i.e., the amplitude U of the L mode decreases exponentially with time t. Thus, in cytosol the axisymmetric L mode of MTs is generally a free vibration with significant damping.

Furthermore, at small k, $\Omega^2-M_{nk}\Omega-\alpha=0$ can also be obtained from Eq. (10). In the absence of cytosol, i.e., $M_{nk}=0$, this equation yields $\Omega=\sqrt{\alpha}$ which gives the dispersion relation for the axisymmetric R mode (Fig. 2). In the presence of cytosol the solution of the equation is $\Omega=M_{nk}\pm\sqrt{M_{nk}^2+4\alpha}/2=-Bi$. Our numerical results show that such a solution can be obtained for the R mode throughout the full length of k considered here. Thus, the axisymmetric radial motion of MTs in cytosol is an exponentially decreasing function of time t, i.e., $e^{-(BS_L/R)t}$, which corresponds to an overdamped vibration where only non-oscillatory radial motion is allowed.

3.2. Non-axisymmetric vibrations

In this section we turn to the non-axisymmetric vibration of MTs in cytosol, which is characterized by $n\geqslant 1$. In this case, coupling always occurs among displacements of MTs in longitudinal, circumferential and radial directions. Naturally, the energy dissipation will take place as a result of the MT–cytosol interaction in radial direction and the strong viscous force in cytosol. The phonon-dispersion relations have been derived for the non-axisymmetric vibrations of MTs in cytosol (solid lines) and compared with those of free MTs (dotted lines) in Fig. 3.

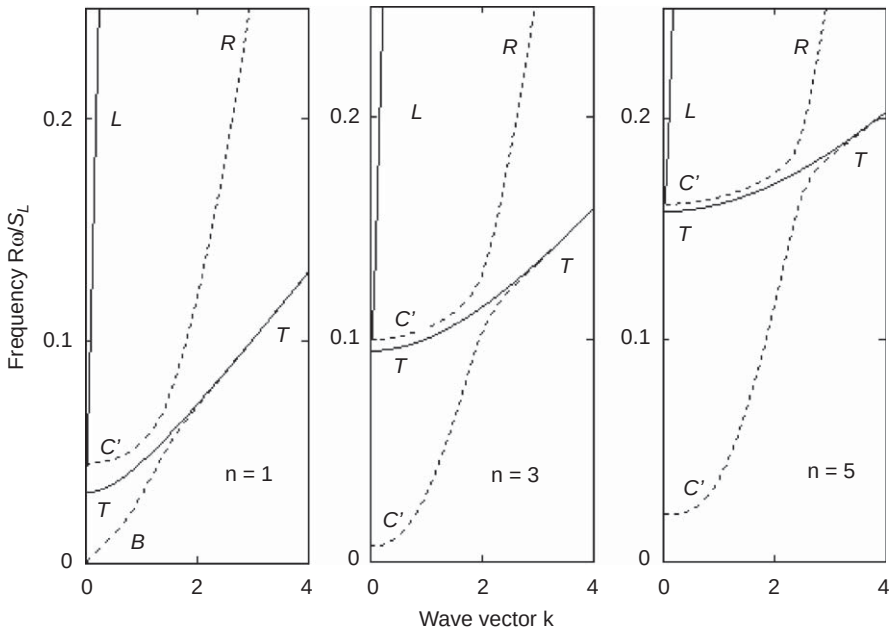

Fig. 3. The phonon-dispersion curves for non-axisymmetric modes of free MTs (dotted lines) and MTs immersed in cytosol (solid lines) with (a) $n=1$, (b) $n=3$ and (c) $n=5$. *L*: longitudinal mode, *T*: torsional mode, *R*: radial mode, *C* and *C'*: circumferential modes and *B*: bending mode. Here, the dotted lines for *L* mode of free MTs coincide with their solid counterparts obtained for MTs in cytosol.

As shown in Fig. 3, for each (n,k) there exist three non-axisymmetrical vibration modes for free MTs. For $n=1$ and $k<1$ the lowest frequency (Fig. 3a) corresponds to the bending (B) mode where MTs bend in tranverse direction with rigid body motion of their circular cross-sections. For $n\geqslant 2$ and $k<1$ the lowest frequency (Fig. 3b and c) is associated with the circumferential (C) modes where the bending of MTs occurs in circumferential direction with distorted (non-circular) cross-sections. In addition, the intermediate frequency gives the C or R mode and the highest frequency corresponds to the L mode of MTs. For MTs in cytosol, Fig. 3 shows that the available non-axisymmetric vibration is limited to L and T modes where longitudinal and circumferential displacements are much greater than the radial one. Similar to the axisymmetric L mode, the solution of Eq. (7) for the non-axisymmetric L and T modes is $\Omega=A-Bi$ $(B>0)$ showing that they are damped vibrations defined by the type of function shown in Eq. (11). As far as the T mode at $k>2$ and L mode are concerned, no visible discrepancy can be found in Fig. 3 between free MTs and those immersed in cytosol. This phenomenon has also been observed in Fig. 2 for axisymmetric L and T modes. It is thus concluded that the major influence of cytosol is to demolish the amplitudes of vibrations that survive in an MT–cytosol system, instead of altering their frequencies.

Stronger damping occurs for B, R and C modes of MTs, whose radial displacements are comparable to or even larger than those in longitudinal and circumferential directions. As shown in Fig. 3, these vibrations obtained for free MTs have been eliminated in an MT–cytosol system. The numerical analysis indicates that Ω obtained in Eq. (7) for these motions is $-Bi$, suggesting that the transverse bending, circumferential bending and radial motions of MTs are non-oscillating motions defined by $e^{-(BS_L/R)\cdot t}$. In particular, the exponential decay of transverse bending has been observed experimentally for MTs in (Felgner et al., 1996), where an MT in a solution was bent by a laser beam and when switching off the laser power it went back to its equilibrium with an exponential decay of its deflection. Such a non-oscillatory bending motion, however, is in sharp contrast to the undamped bending vibration predicted by the shell-ideal fluid model (Sirenko et al., 1996). Thus, the agreement between the present shell-Stokes flow model and the experiment shows that the present model is more realistic, which gives a reliable description for the dynamic behaviours of MTs in cytosol.

As mentioned before, the friction on MT surfaces is small and thus neglected in the present study. The damping effect of cytosol is, therefore, attributed primarily to the MT–cytosol interaction in radial direction, i.e., the motion-induced net pressure $P_{rr}{}^{o}-P_{rr}{}^{i}$ (Eq. (5)) on MTs due to cytosol. This explains why the axiymmetric T mode of MTs decoupled with radial vibration is free from damping, the L and non-axisymmetric T modes coupled with small radial displacements appear as damped free vibrations, and the bending and radial motions of MTs with large radial displacements turn out to be non-oscillatory motions. Here, the relaxation time τ $(=R/BS_L\ \ln 10)$, i.e., the time it takes to reduce the vibration amplitude to one-tenth of its initial value is calculated to measure the damping of L modes and non-axisymmetric T modes. The results show that τ varies from the order of 0.01 ms (10^{-8}) to 10^5 s, and is always three–eleven orders of magnitude greater than the corresponding vibration period. Thus, even with strong damping the L and non-axisymmetric T modes could still exert significant impacts on the mechanical integrity and appropriate functioning of MTs.

4. Conclusion

An orthotropic shell-Stokes flow model has been developed to study the dynamic behaviors of MTs in cytosol. It is found that

(a) Nanoscale MTs give a small Reynolds number ($\sim 10^{-3}$) for the surrounding cytosol flow suggesting the predominant effect of its viscous force. The energy dissipation due to this viscous force is identified as an origin of damping and the strength of damping is largely determined by the motion-induced net radial pressure on MTs.

(b) The axisymmetric torsional vibration decoupled with radial motion leads to zero net pressure on MTs and thus, is free from the damping effect of cytosol. The longitudinal and non-axisymmetric torsional vibrations induce a significant net

pressure on MTs via their small radial components and results in the damped vibrations decaying exponentially with time.

(c) The strongest damping occurs for the transverse or circumferential bending and radial motions of MTs, which result in a high net pressure on the MTs. These motions of MTs turn out to be non-oscillatory motions in cytosol.

The present orthotropic shell-Stokes flow model removes the substantial defects of the previous study (Sirenko et al., 1996) where a fluid surrounding MTs is modeled as an ideal fluid. Specifically, the qualitative agreement between the present model and the experiment (Felnger et al., 1996) in studying the bending motion of MTs shows a clear evidence for the relevance of the present model to the dynamic behaviors of nanoscale tubes immersed in a fluid.

Conflict of interest statement

All authors declare that there are no financial and personal relationships between the present authors and other people or organisations that could inappropriately influence (bias) our research work.

Appendix A. Supporting Information

Supplementary data associated with this article can be found in the online version at doi:10.1016/j.jbiomech.2009.03.027.

References

Boal, D., 2002. Mechanics of the Cell. Cambridge University Press, Cambridge.
Cotterill, R., 2002. Biophysics—An Introduction. Wiley, New York.
dePablo, P.J., Schaap, I.A.T., Mackintosh, F.C., Schmidt, C.F., 2003. Deformation and collapse of microtubules on the nanometer scale. Physical Review Letters 91, 098101–098114.
Felgner, H., Frank, R., Schiwa, M., 1996. Flexural rigidity of microtubules measured with the use of optical tweezers. Journal of Cell Science 109, 509–516.
Gittes, F., Mickey, B., Nettleton, J., Howard, J., 1993. Flexural rigidity of microtubules and actin-filaments measured from thermal fluctuations in shape. Journal of Cell Biology 120, 923–934.
Happel, J., Brenner, H., 1973. Low Reynolds Number Hydrodynamics. Noordhoff International Publishing, The Netherlands.
Howard, J., Hyman, A.A., 2003. Dynamics and mechanics of the microtubule plus end. Nature 422, 753–758.
Ingber, D.E., Prusty, D., Sun, Z.Q., Betensky, H., Wang, N., 1995. Cell shape, cytoskeletal mechanics, and cell cycle control in angiogenesis. Journal of Biomechanics 28, 1471–1484.
Kasas, S., Cibert, C., Kis, A., Rios, P.D.L., Riederer, B.M., Forro, L., Dietler, G., Catsicas, S., 2004. Oscillation modes of microtubules. Biology of the Cell 96, 697–700.
Kurachi, M., Hoshi, M., Tashiro, H., 1995. Buckling of a single microtubule by optical trapping forces—direct measurement of microtubule rigidity. Cell Motility and the Cytoskeleton 30, 221–228.
Nogales, E., 2000. Structural insights into microtubule function. Annual Review of Biochemistry 69, 277–302.
Pokorny, J., 2003. Viscous effects on polar vibrations in microtubules. Electromagnetic Electromagnetic Biology and Medicine 22, 15–29.
Pokorny, J., 2004. Excitation of vibrations in microtubules in living cells. Bioelectrochemistry 63, 321–326.
Portet, S., Tuszynski, J.A., Hogue, C.W.V., Dixon, J.M., 2005. Elastic vibrations in seamless microtubules. European Biophysics Journal 34, 912–920.
Sirenko, Y.M., Stroscio, M.A., Kim, K.W., 1996. Elastic vibration of microtubules in a fluid. Physical Review E 53, 1003–1010.
Stamenovic, D., 2005. Microtubules may harden or soften cells, depending of the extent of cell distension. Journal of Biomechanics 38, 1728–1732.
Venier, P., Maggs, A.C., Carlier, M.F., Pantaloni, D., 1994. Analysis of microtubule rigidity using hydrodynamic flow and thermal fluctuations. Journal of Biological Chemistry 269, 13353–13360.
Watanabe, T., Noritake, J., Kaibuchi, K., 2005. Regulation of microtubules in cell migration. Trends in Cell Biology 15, 76–83.
Wang, C.Y., Ru, C.Q., Mioduchowski, A., 2006a. Vibration of microtubules as orthotropic elastic shells. Physica E 35, 48–56.
Wang, C.Y., Ru, C.Q., Mioduchowski, A., 2006b. Orthotropic elastic shell model for buckling of microtubules. Physical Review E 74, 52901–52914.
Wang, C.Y., Zhang, L.C., 2008. Circumferential vibration of microtubules with long axial wavelength. Journal of Biomechanics 41, 1894.